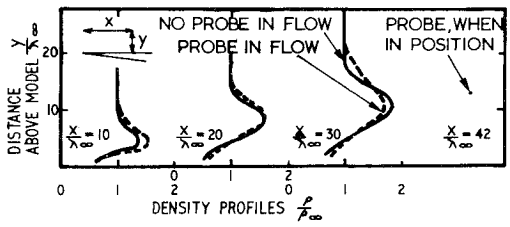

Fig. 1 Effect of transverse probe on density; $\lambda_\infty = 0.38$ mm.

section of the tunnel is highly luminous because of radiative decay of meta stable atoms previously excited in the high temperature arc. It has recently been shown[1] that this luminosity is directly proportional to local gas density. Measurements of luminosity with and without a probe in the flow can therefore be used to assess the extent of the effect of the probe on gas density. Conditions in the working section of the wind tunnel were as follows: Mach number 0(7), static temperature 0(100°C), mean free path λ_∞ 0(1mm). Two probes, typical of those normally used in low density measurements were used for these tests. One probe consisted of a 0.2-mm-diam tungsten wire transverse to the flow. The other probe consisted of a forward facing 1-mm-diam tube supported from beyond the downstream end of the model.

Photographs of the flow about the model were scanned with a photo-densitometer to determine the luminosity and hence the gas density in the flow. The profiles so obtained were reproducible. The process was also applied to photographs taken when one of the probes was present in the flow. Figure 1 shows the effect of the transverse probe. Density profiles were irregularly disturbed, even far upstream of the probe. In Fig. 1 the probe was immediately behind the shock wave which is the position at which maximum flow disturbance occurred. The forward facing probe had a more drastic and erratic effect on density. It was difficult to obtain useful information directly from these disordered profiles and therefore the profiles were used to find the shock position as shown in Fig. 2. It will be seen that the shock moves away from the model when the probe is introduced. This effect is more pronounced when the probe is placed in the faster flow away from the wall, which suggests that the probe is causing blockage. The presence of a small probe in a supersonic boundary layer would not be expected to seriously affect the external shock upstream of the probe. However, as the boundary layer and shock are merged, shock waves are highly sensitive to back pressure so that a substantial change in shock angle may result from the introduction of a probe into the boundary layer.

Conclusions

When probes are introduced into a high-speed rarefied flow, they cause disturbances to the flow structure which are likely to affect the results obtained, even when the probes are near free molecular and very small compared with the extent of the flow being investigated. The use of probes in rarefied flows should, therefore, be confined to the determination of gross features, such as the number and approximate position of shock waves in the flow about complex shapes.

It is emphasized that the profiles obtained from probes may appear to be reasonable. It is only when data obtained from probes causing different amounts of disturbance are combined that anomalies appear. The fact that different probes cause different amounts of disturbance also accounts for the large scatter in the published data for shock position.

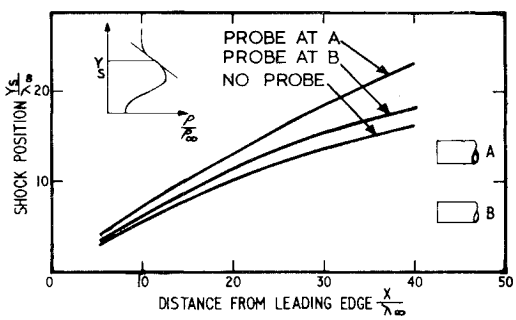

Fig. 2 Effect of forward facing probe on shock position; $\lambda_\infty = 0.38$ mm.

Reference

[1] Cogan, D. M. and Harvey, J. K., "Density Measurements in High Speed Arc-Heated Flows," *Journal of Physics, Ser. E., Scientific Instruments*, Vol. 6, June 1973.

Transonic Flow past Lifting Airfoils

N. R. SUBRAMANIAN* AND M. BALAKRISHNAN†
Indian Institute of Technology, Madras, India

Nomenclature

$c(x)$ = camber distribution
$t(x)$ = thickness distribution
Γ = circulation
$\sigma_E = \dfrac{1}{2\pi(\lambda_E)^{1/2}} \ln\left[(x-\xi)^2+\lambda_E(z-\zeta)^2\right]$
$\Delta\,\partial\phi/\partial\zeta = (\partial\phi_u/\partial\zeta)-(\partial\phi_1/\partial\zeta)$
$\Delta\phi = \phi_u-\phi_1$
$\dfrac{\partial\sigma_E}{\partial x} = \dfrac{1}{2\pi(\lambda_E)^{1/2}} \dfrac{(x-\xi)}{\left[(x-\xi)^2+\lambda_E(z-\zeta)^2\right]}$
$f_E = \{\lambda_E-(K+\gamma+1)\phi_x\}\,\partial u/\partial\xi$
$\lambda_E = [K-(\gamma+1)\phi_x]$

Subscripts
E = elliptic type solution (subsonic case)
u = upper surface
1 = lower surface

DURING the last decade quite a few powerful methods both numerical and analytical have been developed[1] to solve the nonlinear transonic flow equation, in order to obtain the pressure distribution around airfoils. Among the approximate techniques may be cited the 1) hodograph method, 2) parabolic method, and 3) integral equation method. Nieuwland[2] in 1967 developed an indirect method for the potential flow around a family of quasi-elliptical airfoils based on hodograph techniques and the solutions of the hodograph equation are found for a given Mach number and a certain airfoil shape results. If a Mach number dependent parameter is changed, the airfoil shape gets altered. In this way shock free airfoils have been obtained whose uniqueness still appears to be doubtful. Numerical techniques have also been formulated by Steger and Lomax,[3] who have developed finite-difference schemes using a mixed finite-difference system both for lifting and nonlifting airfoils and have obtained interesting results. These sophisticated methods involve high-speed computers. In spite of these numerical methods there is still a need for simple engineering approximation useful for the aircraft designer. The method of local linearization developed by Spreiter et al.[4] continues to be sufficiently precise for quick evaluation. To the authors' knowledge, this technique does not

Received April 27, 1973; revision received June 4, 1973.
Index category: Subsonic and Transonic Flow.
* Professor, Department of Aeronautical Engineering.
† Lecturer, Department of Applied Mechanics. Member AIAA.

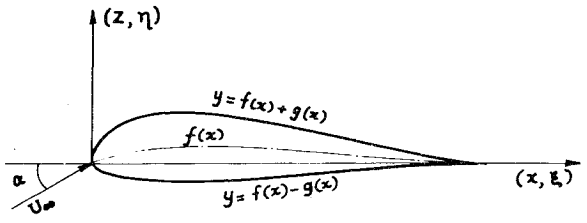

Fig. 1 Lifting airfoil geometry.

appear to have been extended to lifting airfoils. The object of this Note is to extend the technique to lifting airfoils and to compare the results with experimental results by Knechtel[5] obtained in interference-free wind tunnel.

Fundamental Equations and Boundary Conditions

Consider the steady flow of an inviscid, nonheat-conducting compressible gas past an arbitrary thin cambered lifting airfoil, as illustrated in Fig. 1. For small angles of attack, it can be shown by singular perturbation analysis, that the governing partial differential equations for transonic flow take the form

$$[Ku-(\gamma+1/2)u^2]_x+w_{\bar z}=0 \tag{1}$$

$$-w_x+u_{\bar z}=0 \tag{2}$$

Where u and w are the perturbation velocities in the x and $\bar z$ directions and $K=(1-M^2)/\tau^{2/3}$ (τ is the thickness ratio $\bar z=\tau^{1/3}z$). The second equation shows that the flow is irrotational to the first order of approximation and hence a velocity potential can be introduced $(u, w)=\text{gred}\,\phi(x,\bar z)$. Equation (1) can be written as

$$\text{or}\qquad \begin{aligned}&\{K\phi_x-[(\gamma+1)/2]\phi_x^2\}_x+\phi_{\bar z\bar z}=0\\ &[K-(\gamma+1)\phi_x]\phi_{xx}+\phi_{\bar z\bar z}=0\end{aligned} \tag{3}$$

Boundary conditions for Eq. (3) are

$$w(x,0+)=[c'(x)-\alpha/\tau]+t'(x)$$

$$w(x,0-)=[c'(x)-\alpha/\tau]-t'(x)$$

The Kutta conditions, at the sharp trailing edge $y=0$, $x=1$, are

$$(\phi)_{\text{wake}}=(\phi)_{\bar z=0+}-(\phi)_{\bar z=0-}=\Gamma$$

Velocity perturbations should vanish at upstream infinity. Spreiter develops a method of local linearization for the solution of Eq. (3) for the 3 cases $\lambda=[K-(\gamma+1)\phi_x]\gtrless 0$. Application of Green's theorem to a region $\bar R_E$ surrounding the wing and wake as illustrated in Fig. 2 and an a priori assumption regarding the attenuation of the disturbances over a large circle leads to the following integral equation for $\phi(x,\bar z)$ for the purely subsonic flow ($\lambda=\lambda_E>0$):

$$\phi(x,\bar z)=\int_0^\infty\left(\sigma_E\frac{\Delta\,\partial\phi}{\partial\zeta}-\Delta\phi\frac{\partial\sigma_E}{\partial\zeta}\right)d\xi+\iint_{\bar R_E}\phi_E f_E\,d\bar R \tag{4}$$

The first term in the integral equation involves a distribution of sources σ_E proportional to $\Delta(\partial\phi/\partial\zeta)$ and doublets $d\sigma_E/d\zeta$ proportional to $\Delta\phi$ with $\Delta(\partial\phi/\partial\zeta)=2t_x$. The contribution is zero for the thickness distribution.

$$\phi(x,\bar z)=2\int_{-1}^{1}\sigma_E t_x\,d\xi-\int_0^\infty\Delta\phi\frac{\partial\sigma_E}{\partial\zeta}d\xi+\iint_{-\infty}^{+\infty}f_E\sigma_E\,d\xi\,d\zeta \tag{5}$$

$$u(x,\bar z)=2\int_{-1}^{1}\frac{\partial\sigma_E}{\partial x}t_x\,d\xi\frac{\partial}{\partial x}\int_0^\infty\Delta\phi\frac{\partial\sigma_E}{\partial\zeta}d\xi+\iint_{-\infty}^{+\infty}f_E\frac{\partial\sigma_E}{\partial x}d\xi\,d\zeta \tag{6}$$

The method adopted in the present Note is essentially the technique of local linearization, extended to the lifting case. To improve upon the accuracy of the first approximation, λ instead of being equated to K is equaled to $[K-(\gamma+1)u(x,\bar z)]$ in which case the double integral of the integral equation reduces to

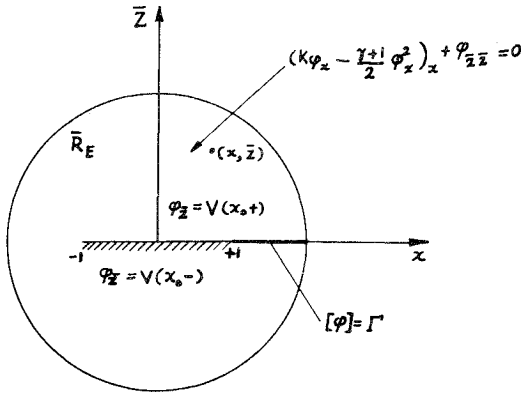

Fig. 2 Boundary value problem for plane transonic flow.

$(\gamma+1)[u(x,\bar z)-u(\xi,\zeta)]\,\partial u/\partial\xi$ which vanishes at the point $\xi=x$, $\zeta=\bar z$ where σ_E, $\partial\sigma_E/\partial x$ and $\partial^2\sigma_E/\partial x^2$ are infinite, and only the contribution from the single integral results. The incidence problem is solved by superposing on the nonlinear thickness effects obtained by Spreiter, a nonlinear incidence solution, obtained by a doublet distribution on the mean chord line but forcing f_E to zero at the point where $\partial^2\sigma_E/\partial x^2$ is infinite

$$C_p=\frac{-2}{(\gamma+1)M_\infty^{\,2}}\{(1-M_\infty^{\,2})-[(1-M_\infty^{\,2})^{3/2}+$$

(for thickness problem) $$\tfrac{3}{4}M_\infty^{\,2}(\gamma+1)C_{p_i}]^{2/3}\} \tag{7}$$

Where C_{p_i} is the incompressible pressure distribution obtained by linear theory. The pressure distribution on circular arc airfoils has been computed for thickness ratio of 6%, Mach numbers ranging from 0.706 to 0.711 and angles of attack 1°, 2°, 3° and 4° and compared with wind-tunnel results provided by Knechtel, in Figs. 3 and 4.

Discussion

At small angles for $M_\infty=0.706$ (Fig. 3) the comparison between theoretical and the experimental results is very satisfactory. At larger angles of attack of the order of 4°, the distribution at the lower surface appears to compare well with the experimental values while at the top surface it is less satisfactory. This discrepancy might be due to the large expansion taking place near the leading edge, as well as the viscous effects. It is possible that the agreement can be made to improve by a process of quadratic iteration following the lines of Spreiter for the thickness case. The method of approach would be to feed in the results of the present approach as starting values and refining them by an iteration process.

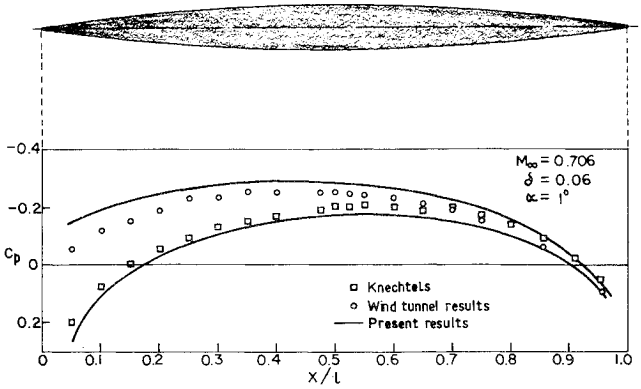

Fig. 3 Pressure distribution on circular arc airfoils at incidence at transonic speed.

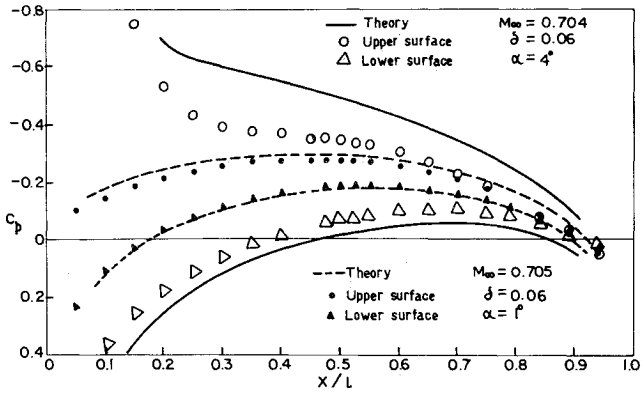

Fig. 4 Pressure distribution on circular arc airfoils at incidence at transonic speed.

References

[1] *Symposium Transsonicum,* edited by K. Oswatitsch, Springer Verlag, Gottingen, 1962.

[2] Nieuwland, G. Y., "Transonic Potential Flow around a Family of Quasi-Elliptical Aerofoil Sections, NLR TR T 172, 1967, National Lucht-en-Ruimtevaart Laboratorium.

[3] Steger, J. L. and Lomax, H., "Generalized Relaxation Methods Applied to Problems in Transonic Flow," *Lecture Notes in Physics,* Vol. 8, edited by J. Ehlers et al., Springer Verlag, Berlin, 1971, pp. 194–197.

[4] Spreiter, J. R. and Alksne, A. Y., "Thin Airfoil Theory Based on Approximate Solution of the Transonic Flow Equation," Rept. 1359, 1958, NACA.

[5] Knechtel, E. D., "Experimental Investigation at Transonic Speeds of Pressure Distributions over Wedge and Circular Arc Airfoil Sections and Evaluation of Perforated Wall Interference," TN D-15, 1959, NASA.

Isoperimetric Formulation for Some Problems of Optimization of the Entry into Atmosphere

AL MARINESCU*
Institute of Fluid Mechanics and Aerospace Constructions, Bucharest, Romania

Nomenclature

z = altitude
x = distance upon horizontal
ρ = density = $\rho_0 e^{-\beta z}$
S = reference surface
S_v = area of the vehicle surface
V = velocity of the vehicle
C_z = lift coefficient
C_x = drag coefficient
θ = inclination angle of the trajectory with respect to the local horizontal
m = vehicle mass

Introduction

THE optimization of the entry of space vehicles into the planetary atmosphere constitutes at the present time the object of many preoccupations. In this respect author's paper[1] gives a formulation that may be generalized to several entry problems.

In principle we refer to the problems of the minimum time lifting entry, the lifting entry with minimum total heat yielded to the vehicle, the lifting entry with minimum consumption of ablative mass and the lifting entry with minimum heat yielded in the critical zone. The present Note approaches briefly two problems, the others being only mentioned.

In all cases it is assumed that the entry is made on a plane trajectory at small initial angles and the lift differs from zero, the angle θ being considered positive in the descent.

The governing motion equations are

$$dV/dt = -(SC_x/2m)\rho V^2; \quad dz/dt = -V\sin\theta$$
$$d\theta/dt = -(SC_z/2m)\rho V; \quad dx/dt = V\cos\theta \tag{1}$$

Minimum Time Optimal Lifting Entry into Planetary Atmosphere

In the following we determine the optimal laws of variation of the motion parameters such that a lifting vehicle should travel the descending trajectory between the altitudes z_i, z_f in the shortest time, the distance on the horizontal being given.

We introduce the variable z such that the two first equations (1) become

$$dV/dz = (SC_x/2m)\rho V/\sin\theta$$
$$d\theta/dz = (SC_z/2m)\rho/\sin\theta \tag{2}$$

From the first Eq. (2), denoting $dV/dz = V'$ and $SC_x/2m = a$ we have

$$\sin\theta = a\rho V/V' \tag{3}$$

Taking account of the third Eq. (1) and Eq. (3) the time in which the vehicle travels the discending path between the altitudes z_i, z_f becomes

$$t = \frac{1}{a}\int_{z_f}^{z_i} \frac{V'}{\rho V^2}dz \tag{4}$$

From the third and fourth Eq. (1), by expressing ctg θ function of sin θ as shown in[1] we have

$$x = \int_{z_f}^{z_i}\left(\frac{1}{a\rho V/V'} - \frac{a\rho V}{2V'}\right)dz \tag{5}$$

The variational problem which confronts us now is to find the minimum of the functional (4) with the condition $x = l$, where l is a given length. As it may be seen, the variational problem is an isoperimetric problem with a moving extremity, since the velocity is not indicated for the final altitude z_f.

The curve which achieves the extremum of the functional (4) is an extremal of the functional

$$J = \int_{z_f}^{z_i} H\,dz \tag{6}$$

where

$$H = V'/\rho V^2 + \Lambda[(1/a)V'/\rho V - (a/2)\rho V/V'] \tag{7}$$

Λ being a constant.

Taking account of Eq. (7) and of the exponential variation of the density and setting $\Lambda = a\lambda$, Euler's equation leads to the differential equation

$$V'' + \frac{\beta}{2}V' - \frac{V'^2}{V} - \frac{\beta V'^3}{a^2\rho^2 V^2}\left(1 + \frac{1}{\lambda V}\right) = 0 \tag{8}$$

It may be demonstrated with the aid of Legendre and Weierstrass' conditions that the extremal of the problem $V(z)$, solution of Eq. (8), achieves indeed the minimum with constraints of the functional (4).

Equation (8) may be transposed into the system $dV/dz = V'$

$$\frac{dV'}{dz} = -\frac{\beta}{2}V' + \frac{V'^2}{V} + \frac{\beta V'^3}{a^2\rho^2 V^2}\left(1 + \frac{1}{\lambda V}\right) \tag{9}$$

which is numerically integrated as shown in Ref. 1.

With the optimal law of variation of the velocity previously deduced we determine the law variation of the angle θ. Dividing Eqs. (2), considering $C_z/C_x = \text{const}$ and integrating with the

Received May 24, 1973.
Index category: Entry Vehicle Dynamics and Control.
* Senior scientist.